Efficient Uranium (VI) Extraction from Aqueous Solutions Using Commercial Anion Exchange Resin: Advanced Analysis of Kinetics, Adsorption Models, and Thermodynamic Behavior

El Sayed A Haggag, Walid M Youssef, Ahmed M Masoud, Ahmed E M Hussein, Mahmoud M Elmaadawy, Mohamed H Taha, and Yasser M Khawassek

Nuclear Materials Authority, P.O. Box 530, El Maddi, Cairo, Egypt.

Abstract: This study explores the efficient extraction of uranium (VI) from aqueous solutions using the marketable strong anion exchange resin, MTA6002PF, provided by Purolite. The research examines the sorption process by focusing on kinetics, adsorption isotherms, and thermodynamic behavior. The resin displayed consistent performance in terms of both kinetic and isotherm properties, with a capacity of around 71 mg/g. The progression was determined to be endothermic, viable, and spontaneous, with uranium (VI) elution reaching up to 95% when consuming 1.0 M sulfuric acid. Despite the complex composition of leach liquor from Egyptian samples, the resin showed excellent sorption efficiency. These findings emphasize the potential of MTA6002PF as a reliable and operative material for uranium recovery from acid solutions, offering valuable insights into the optimization of uranium extraction in industrial settings.

1. Introduction

Nuclear-powered energy is widely acknowledged as a clean and renewable power source, acting a vital role in fulfilling global energy needs while mitigating greenhouse gas emissions [1]. However, the extraction and processing of uranium, the prime fuel used in nuclear energy production, result in obtaining of significant quantities of uranium-laden wastewater. This wastewater presents a major environmental concern, as inadequate handling can lead to contamination of water resources and ecosystems [2, 3]. As a consequence, there is a crucial need to develop effective and sustainable means for extracting uranium (VI) from aqueous solutions, including those resulted throughout uranium ore mining, processing, tailings management, and from natural sources such as lake waters [3].

Numerous methods have been investigating for extracting uranium (VI) from leach solutions, comprising precipitation [4], ion exchange [5], solvent extraction [6], catalytic processes [7], and adsorption [8]. Among these techniques, adsorption is considered one of the furthermost operative due to its simplicity, cost-efficiency, and capacity to take out uranium ions even at low-slung concentrations without producing secondary pollutants [1, 2]. A broad range of adsorbents were investigated for uranium removal, such as carbon-based materials [8], functionalized fiber materials [9], hydrogels, magnetic nanoparticles [8], metal organic frameworks (MOFs), and covalent organic frameworks (COFs) [10]. However, many of these materials have limitations, including poor chemical stability, low

adsorption efficiency at low uranium concentrations, complex synthesis procedures, and elevated costs, in which hinder the practical usage for large-scale uranium recovery from wastewater or seawater.

To overcome these challenges, there is increasing interest in utilizing anion exchange resins, which are known for their high adsorption capacity, fast kinetics, and ease of regeneration. Many commercially available resins, including Amberlite IRA-400 [11], Amberlite IR120 [12], C100H resin [13], and Amberjet 1200 H [14], have been investigated for uranium recovery. These resins have shown promising performance in treating uranium-laden leach liquors, positioning them as viable options for industrial applications.

This study inspects the use of commercially offered ion exchange resin, particularly MTA6002PF, for the uranium (VI) extraction from acidic sulfate solutions. The main objectives are to examine the factors affecting uranium adsorption, comprising pH, uranium concentration, contact time and reaction temperature, along with to assess the kinetic, isotherm, and thermodynamic characteristics of the sorption process. By optimizing these parameters, the research aims to offer valuable perceptions into the practical usage of anion exchange resins for efficient uranium recovery from complex aqueous solutions.

2. Experimental

2.1. Materials

The MTA6002PF anion exchange resin, provided by Purolite (King of Prussia, PA, USA), is a strong base resin designed for uranium recovery from acidic solutions. The resin's key chemical and physical characteristics are detailed in Table 1. Before use, the resin was pre-conditioned through washing by means of deionized water to take away impurities and converting it to the sulfate form to improve its sorption efficiency. For resin activation and uranium desorption, analytical-grade reagents such as HCl, H₂SO₄, and HNO₃ (Sigma-Aldrich, USA) were utilized. Uranium solution (1000 mg/L) was ready using uranyl sulfate salts and diluted as necessary. To maintain the pH, 0.1 M of each NaOH and HCl were utilized, with distilled water used to ensure the experiments accuracy.

2.2. Synthesis of leach liquor solution

Uranium(VI) extraction experiments were carried out using sulfate leach liquor obtained from El-Erediya uranium(VI) ore-sample from Eastern Desert, Egypt. The leaching process was performed under controlled conditions to optimize uranium dissolution [15]. The sample was powdered to an adequate particle size of 63 µm and leached with 1.5 M sulfuric acid (H₂SO₄) at an ore-to-acid ratio (1:3). The mix was agitated at 600 rpm aimed at two hours at ambient temperature, through addition of 1.0 M hydrogen peroxide (H₂O₂) to enhance uranium oxidation and increase its solubility. After the leaching process, the resulting solution was filtered to eliminate solid residues. The concentration of uranium in the leachate was measured by means of a UV-visible spectrophotometer (UV SP-8001, Metretech Inc.), with Arsenazo III serving as the indicator. The composition of the sulfate leach liquor is outlined in Table 2.

2.3. Batch investigation

The adsorption test was implemented in a batch reactor to consider the effectiveness of uranium (VI) removal from aqueous solutions. A fixed solution volume (V, L) with an original uranium conc. (C₀, mg/L) was combined with a set amount of resin (m, g) and continuously stirred by 150 rpm for 10 hours to achieve equilibrium. The sorbent dose was generally maintained at 1.0 g/L, although variations between 0.2 and 1.2 g/L were tested to observe their influence on sorption efficiency. The preliminary uranium concentration (C₀) was in the range of 20 - 160 mg/L to explore the sorption isotherms. After the sorption process, the solution was filtered by means of a membrane through a 1.2 μm pore size, and the remaining uranium concentration (C_e, mg/L) was evaluated via a modified Davies and Gray titrimetric method and spectrophotometric analysis. The distribution constant (K_d), the sorption

capacity (qe, mg/g), and the adsorption efficiency (R%) were then enumerated using the subsequent equations:

$$K_d = \frac{(C_o - C_e)}{C_e} X \frac{v}{m} \dots (1)$$

$$q_e = (C_o - C_e)X \frac{V}{m}....(2)$$

$$R \% = \frac{(C_o - C_e)}{C_o} X 100....(3)$$

2.4. Modeling of sorption process

To gain a more comprehensive thoughtful of the uranium (VI) adsorption process, the investigational data were examined through kinetic, isotherm, and thermodynamic models. These models help to point out the adsorption rate, the equilibrium behavior of the system, and the thermodynamic feasibility of the process.

2.4. 1. Adsorption kinetic models

The adsorption kinetics of uranium were analyzed to estimate the rate and mechanism of the sorption process. Three kinetic models were employed in this analysis [16]:

2.4.1.1. Pseudo first order equation (PFO). The PFO, developed by Lagergren, explains the adsorption rate under the assumption that it is proportionate to the numeral of available adsorption sites. The nonlinear expression of the PFO model is represented by [16].

$$q_t = q_1(1 - e^{-k1t}) \dots (4)$$

Where $k1 \text{ (min}^{-1})$ is Largergren equation rate constant, and $q_1 \text{ (mg g}^{-1})$ is the predictable adsorption capacity by PFO model.

2.4.1.2. Pseudo second order equation (PSO). The PSO, likewise recognized as the McKay equation, assumes that chemisorption is the rate-limiting step. The PSO model non-linear form is assumed by [16]:

$$q_t = \frac{1}{(1|k_2q_2^2) + (t|q_2)} \dots \dots (5)$$

 $q_t = \frac{1}{(1|k_2q_2^2) + (t|q_2)} \dots \dots (5)$ The half equilibrium time, $t_{1/2}$ (h), and the preliminary adsorption rate, h (mol g⁻¹ h⁻¹)was attained from equations 6 and 7.

$$t_{1/2} = \frac{1}{k_2 q_e} \dots \dots (6)$$

 $h = k_2 q_e^2 \dots \dots (7)$

 $t_{1/2} = \frac{1}{k_2 q_e} \dots \dots (6)$ $h = k_2 q_e^2 \dots \dots (7)$ Where q_2 (mg g⁻¹) is the predictable adsorption capacity by PSO model, and k_2 (min⁻¹) is the McKay equation rate constant.

2.4.1.3. Intra particle diffusion equation (IPD). The IPD, formulated by Weber & Morris, describes the sorption process as a multi-stage mechanism that includes film diffusion, surface diffusion, and pore diffusion. The IPD equation is expressed as:

$$a_t = K_{id} t^{0.5} + C_{i...}$$
 (8)

 $q_t = K_{id} t^{0.5} + C_i \dots (8)$ where *C* is the boundary layer thickness, and K_{id} (mg g⁻¹. min^{-0.5}) is the rate constant.

2.4.2. Adsorption isotherm models

The equilibrium comportment of uranium (VI) adsorption was analyzed using three isotherm models: Freundlich, Langmuir, and Sips [16].

2.4.2.1. Freundlich isotherm equation. The Freundlich model labels adsorption on heterogeneous surfaces, assuming an exponential distribution of adsorption sites. The non-linear form of the Freundlich equation is:

$$q_e = K_F C_e^{1/n_F} \dots \dots (9)$$

where, $1/n_F$ refer to the adsorbate sites heterogeneity and K_F (mg g⁻¹) is consistent to the Freundlich constant.

2.4.2.2. Langmuir isotherm model. The Langmuir model adopts monolayer adsorption onto a homogeneous surface through no interaction between adsorbed molecules. The nonlinear form of the Langmuir equation represented as:

$$q_e = \frac{q_m k_L C_e}{1 + k_L C_e} \dots \dots (10)$$

where q_m (mg/g) is the max. sorption capacity of the practical resins, and k_L (L. mg⁻¹) is the Langmuir constant in which, denotes to the adsorption energy and give thought to the affinity of resin concerning the metal ions.

2.4.2.3. Sips isotherm equation. The Sips model encompass features of the Langmuir and Freundlich models, making it suitable for describing adsorption on the heterogeneous surfaces. The non-linear form for the Sips equation is:

$$q_e = \frac{q_S(k_S C_e)^{mS}}{1 + (k_S C_e)^{mS}} \dots \dots (11)$$

 $q_e = \frac{q_S(k_S C_e)^{mS}}{1 + (k_S C_e)^{mS}} \dots \dots (11)$ where mS is Sips constant, K_S (L/mg) signifies the constants of Sips model, and q_S is the max. sorption capacity (mg. g-1) of Sips model.

2.4.3. Fitting the kinetic and isotherm models

The goodness of fit for the isotherm and kinetic models was assessed using the non-linear regression chi-square (χ^2) , and the coordination coefficient (R^2) values. These parameters were calculated using the following equations [18]:

Coordination coefficient
$$(\mathbf{R}^2) = 1 - \frac{\sum_{1}^{X} (q_{exp} - q_{pred})^2}{\sum_{1}^{X} (q_{exp} - \overline{q_{exp}})^2} \dots \dots (12)$$

$$x^2 = \sum_{1} \left[\frac{(q_{exp} - q_{pred})^2}{q_{pred}} \right] \dots \dots (13)$$

where q_{exp} is the experimental equilibrium capacity (mg g⁻¹), and q_{pred} is the predicted equilibrium capacity (mg g⁻¹) correspondingly, R^2 and x^2 are the coordination, and Chi-square coefficients correspondingly, and n is the number of test points.

2.4.4. The adsorption thermodynamics.

The thermodynamic conduct of the adsorption process was investigated by analyzing the connection between the adsorption capacity and temperature. The Gibbs free energy change ($\Delta G \circ$), enthalpy change ($\Delta H \circ$), and entropy change ($\Delta S \circ$) were considered using the subsequent equations [18]: $\log K_C = -\frac{\Delta H^o}{2.303 \, R} \, X \, \frac{1}{T} + A \dots (14)$

$$log K_C = -\frac{\Delta H^o}{2.303 R} X \frac{1}{T} + A \dots (14)$$
$$-\Delta G^o = 2.303 RT log K_C \dots (15)$$
$$\Delta G^o = \Delta H^o - T \Delta S^o \dots (16)$$

Where **R** is the universal gas constant (8.314 J mol $^{-1}$. K⁻¹), T is the temperature (K), K_C is a non dimensional equilibrium constant and it equals $K_d \times 1000 \times \rho$; ρ is the solution density g/L, and A considered as a constant.

3. Results and Discussions

3.1. The pH Impact

The solution pH is a critical factor in the adsorption process as it influences mutually the surface charge of the adsorbent and the speciation of uranium (VI) ions. To inspect the pH effect on the uranium adsorption, experimentations were performed with the MTA6002PF resin within a pH range of 1 to 5. The tests were carried out under controlled conditions; a reaction time of 240 minutes, ambient

temperature, initial uranium Conc. of 50 mg/L, and a sorbent dosage of 1 g/L. The outcomes, elucidated in Figure 1, show that the uranium (VI) adsorption efficiency increased as the pH rose, accomplished max at pH 4.0. At this pH, the MTA6002PF resin exhibited a sorption efficiency of 91.2%, corresponding to a sorption capability of 45.6 mg/g. However, as the pH exceeded 4.0, the adsorption efficiency began to decline, suggesting that higher pH levels hinder the sorption process. This pattern suggests that pH 4.0 is the optimal condition for uranium adsorption using the MTA6002PF resin. The detected behavior can be attributed by the changes in the speciation of uranium with respect to pH, as shown in Figure 2. In acidic conditions (pH < 4), the dominant uranium species include UO₂²⁺, UO₂SO₄, and UO₂(SO₄)₂²⁻. At lower pH levels, the positively charged UO₂²⁺ ions are repelled by the resin's cationic sites, driving to a decrease in adsorption efficiency. By way of the pH increases, the concentration of UO₂(SO₄)₂²⁻ complexes increases, which enhances the electrostatic attraction to the resin's active sites, thereby improving uranium adsorption. However, at pH values above 4, the formation of UO₂(OH)₂·H₂O and other hydroxide complexes reduces the availability of uranium species for adsorption, resulting in a decrease in sorption efficiency.

Figure 2, generated using the Medusa/Hydra program, affords a detailed speciation diagram of uranium in 0.1 M H₂SO₄ as a function of pH. The diagram confirms that UO₂²⁺ is the predominant species at low pH (0–2), while UO₂(SO₄)₂²⁻ becomes dominant in the pH range of 2–6. Above pH 6, uranium hydroxide complexes such as UO₂(OH)₂·H₂O, UO₂(OH)₃⁻, and UO₂(OH)₄²⁻ begin to form, which are less satisfactory for adsorption on the resin. These outcomes point out the importance of optimizing the solution pH to maximize uranium adsorption efficiency. The results suggest that a pH of 4.0 is optimal for uranium recovery using the MTA6002PF resin, providing a sense of balance between favorable uranium speciation and resin surface properties.

3.2. Impact of contact time and reaction kinetics

The interaction time between the adsorbent and the solution is a key factor in the adsorption progression, influencing how quickly equilibrium is reached. To assess the guidance of contact time on uranium (VI) adsorption, tests were achieved with the MTA6002PF resin over a time range of 5 to 240 minutes. The experiments were performed under consistent conditions: sorbent prescribed amount of 1.0 g/L, initial uranium Conc. of 50 mg/L, temperature of 298 K, and solution pH of 4.01. As shown in Figure 3, uranium adsorption arose rapidly in the initial stages, reaching near-equilibrium within 60 minutes, with a sorption efficiency of approximately 91.2%. After 60 minutes, the adsorption rate decreased significantly, with no further increase in sorption efficiency. This performance can be due to the availability of active sites onto the resin surface. During the initial phase, a high number of active sites are accessible for uranium ions, resulting in quick adsorption. As these sites become occupied, the adsorption rate slows, and the system approaches to the equilibrium.

To obtain a deeper comprehension of the adsorption kinetics, the experimental information were interpreted using two commonly used kinetic models: the pseudo first order (PFO) and pseudo second order (PSO) models. These models were exercised to help identify the rate determining step and better understand the adsorption processes. While the PFO model provided some insight into the early stages of adsorption, it did not effectively describe the entire sorption process. This was evident from its lower correlation coefficient (R²) and higher chi-square (χ^2) values compared to the PSO model. The difference in model performance suggests that the PFO model oversimplifies the adsorption mechanism, failing to capture the more complex interactions between U(VI) ions and the resin surface. In contrast, the pseudo second order (PSO) model showed a much better fitting to the investigational data. As illustrated in Figure 4 and Table 3, the PSO model provided a high correlation coefficient (R² = 0.99) and a low chi-square value (χ^2 = 0.05), indicating strong consistency with the experimental observations. Furthermore, the predictable adsorption capacity (q²) derived from the PSO model thoroughly harmonized the value observed experimentally, further supporting its effectiveness in describing the adsorption kinetics. The tremendous fit of the PSO model advocates that the adsorption

process is primarily controlled by chemisorption, which includes the exchange or transfer of electrons amongst the functional groups on the resin and the uranium ions. This mechanism aligns with the electrostatic interactions and surface complexation typically seen in anion exchange processes. The attainment of the PSO model in capturing the adsorption kinetics emphasizes the consequence of chemical exchanges in the adsorption process. The initial rapid adsorption phase, as shown in Figure 3, could be assigned to the availability of active sites on the resin surface, in which allows for the quick attachment of uranium ions. As these sites fill up, the rate of adsorption slows, and the system reaches equilibrium [18]. Along with the PFO and PSO models, the IPD model was employed to further explore the diffusion mechanisms involved in the adsorption process [17]. The results from the IPD analysis, presented in Figure 5 and Table 4, revealed that the adsorption progression could be allocated into two distinct stages. The initial stage is characterized by speedy adsorption on the surface, where uranium ions quickly bind to the active sites on the outer surface of the resin. This stage is primarily controlled by the availability of active sites and the strength of the interaction among the resin and the uranium ions [19]. The subsequent stage involves slower intraparticle diffusion, where uranium ions gradually diffuse into the resin's internal pores. This phase is affected by influences such as the pore size, surface area, and the internal structure of the resin [19]. The multi-linear pattern of the IPD plot, as shown in Figure 5, effectively demonstrates the two distinct phases of the adsorption process. The initial linear segment corresponds to the fast surface adsorption phase, where the adsorption rate is rapid due to the plentiful active sites. The subsequent linear segment reflects the slower intraparticle diffusion phase, where the rate of adsorption declines as uranium ions penetrate deeper into the resin's pores [19]. The slope of each segment signifies the rate constant for each phase, with the first phase having a higher rate constant than the second. The IPD model's ability to characterize the adsorption process in these two stages provides valuable insights into the mechanisms at play. The initial rapid adsorption phase suggests strong surface interactions, such as chemisorption, in which uranium ions form chemical bonds with the functional groups of the resin. Meanwhile, the slower diffusion phase highlights the movement of uranium ions through the resin's porous network, a process that can be constrained by factors like pore size and internal resistance.

3.3. The effect of initial concentration of the metal ion

The metal ions initial Conc. in a solution significantly constrains the adsorption process, affecting both the removal efficiency and the resin's capacity. To explore this influence, uranium sorption experiments were carried out using MTA6002PF resin at varying U(VI) concentrations from 20 to 160 mg/L, with a constant sorbent dose of 1 g/L, room temperature, and a contact duration of 120 minutes. As demonstrated in Figure 6, the uranium removal efficiency diminished as the initial Conc. increased, dropping from 96.0% at 20 mg/L to 45.6% at 160 mg/L. This reduction could be due to the saturation of the resin's active sites, which limits the adsorption of additional uranium ions at higher concentrations. However, the resin's uptake capacity increased with the metal ion concentration, peaking at an adsorption capacity of approximately 68.4 mg/g. To further examine the adsorption behavior, the investigational data were formfitting to the following isotherm models: Langmuir, Freundlich, and Sips. The isotherm curve is exposed in Figure 7, and the corresponding parameters are tabulated in Table 5. The results presented in Table 5 point to that both the Langmuir and Sips models offered the finest fit for the investigational data. The Langmuir model, which adopts monolayer adsorption on a uniform surface, yielded a max. adsorption capacity (q_m) of 70.2 mg/g with a high correlation coefficient (R² = 0.99). This result proposes that uranium adsorption on the MTA6002PF resin predominantly occurs through monolayer coverage, where each adsorption site maintains a constant activation energy. The Sips model, which associates elements of both the Langmuir and Freundlich models, also showed a strong fit, reinforcing the idea that the adsorption process involves a mix of both homogeneous and heterogeneous interactions [19]. Moreover, the Freundlich model provided further insight into the multi-layer adsorption characteristics and the surface heterogeneity of the resin. The adsorption intensity parameter (1/n) from the Freundlich model indicated that uranium adsorption is particularly favorable. The adsorption capacity of the tested resins is presented in Table **6**, alongside an appraisal with the adsorption capacities of other sorbents reported in the previous works. The data indicate that the examined resin exhibit adsorption capacity consistent with those of commonly used resins in previous studies.

3.4. Impact of sorbent dose

The sorbent dose plays a key role in determining uranium adsorption efficiency, as it directly influences the numeral of active binding sites available for metal ion uptake. To investigate this effect, experiments were conducted by changing the sorbent dose among 0.2 and 1.2 g/L, while keeping the initial U(VI) concentration at 50 mg/L, maintaining room temperature, and using a shaking time of 120 minutes. As displayed in Figure 8, uranium removal efficiency increased with higher sorbent dosages, reaching a maximum adsorption rate of 93.3% at 1.2 g/L. This tendency can be due to the higher availability of active sites, in which enhances the likelihood of interactions concerning uranium ions and the resin [44].

3.5. The impact of temperature on U(Vl) adsorption

The temperature influence on uranium (VI) adsorption using the MTA6002PF resin was examined to comprehend the thermodynamic aspects of the sorption process. The experimentations were performed over a temperature zone of (20 - 50°C), with fixed parameters including resin prescribed amount (1.0 g/L), initial U(VI) Conc. (50 mg/L), and reaction period (240 minutes). The data were analyzed using thermodynamic equations to generate a Van't Hoff plot (Figure 9) and determine important thermodynamic parameters like the Gibbs free energy change (ΔG°), enthalpy change (ΔH°), and entropy change (ΔS°). The results, summarized in Table 7, demonstrate that the enthalpy change (ΔH°) is positive (14.2 kJ/mol), signifying that the adsorption process is endothermic in nature [17]. This suggests that higher temperatures promote uranium uptake. Furthermore, the negative values of Gibbs free energy change (ΔG°) confirm that the sorption process is spontaneous and thermodynamically favorable. The increasing negativity of ΔG° with rising temperature further supports the idea that uranium adsorption is more efficient at elevated temperatures. The positive entropy change (ΔS°) value (124.6 J/mol·K) indicates a rise in molecular disorder at the solid-solution interface during adsorption, which is consistent with the endothermic nature of the process [17].

3.6. Impact of iron (II) ions concentration

The existence of competing ions in the solution can significantly impact the efficiency of uranium sorption. Iron (II) ions, which are often present in uranium-containing leach liquors, are one of the key competing species. To investigate their effect on uranium adsorption, experiments were conducted by varying Fe(II) concentrations from 0 to 300 mg/L, while keeping the investigational conditions constant (shaking time: 240 min, resin dose: 1.0 g/L, initial U(VI) Conc.: 50 mg/L, room temperature, pH 4.02). As displayed in Figure 10, increasing Fe(II) concentrations led to a decrease in uranium uptake efficiency.

3.7. Scanning Electron Micrograph (Morphology)

To gain insights into the surface properties of the MTA6002PF resin before and afterward uranium adsorption, scanning electron microscopy (SEM) analysis was conducted. The SEM images are shown in Figure 11. The untreated resin (Figure 11-I) exhibits a smooth, uniform spherical shape, indicating a well-defined surface typical of the pristine resin. However, after uranium adsorption, significant changes in the resin's morphology are evident (Figure 11-II).

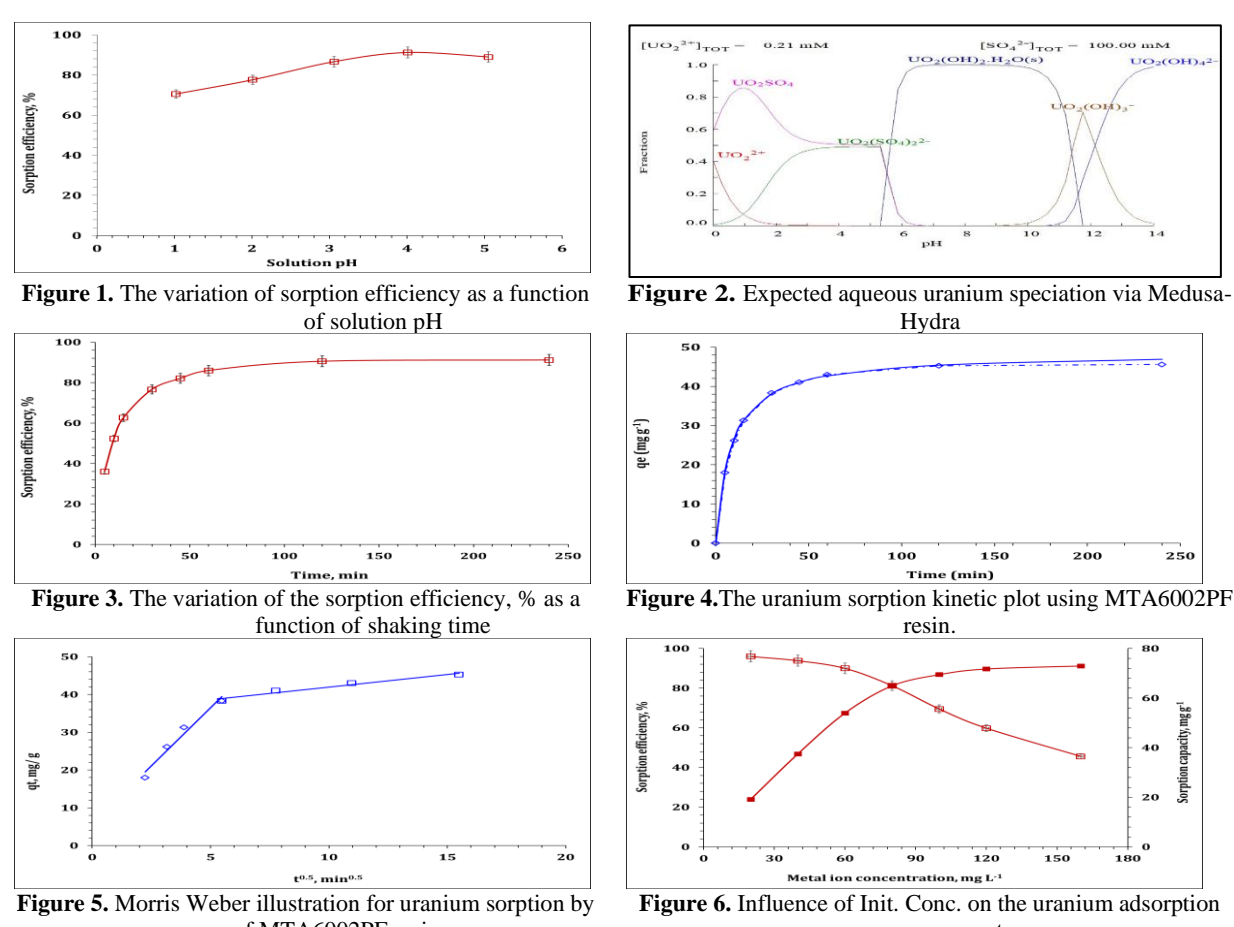
3.9. Elution and recycling investigation

To assess the reusability and desorption efficiency of the MTA6002PF resin, uranium (VI) desorption experiments were conducted using 1.0 M solutions of sulfuric acid (H₂SO₄), nitric acid (HNO₃), and hydrochloric acid (HCl) at ambient temperature. The experiments were performed with a sorbent dosage of 0.5 g/L and a shaking time of 240 minutes. The findings, presented in Table 8, reveal that sulfuric acid resulted in the highest desorption efficiency at 94.0%, followed by nitric acid at 90.2%, and

hydrochloric acid at 86.5%. These results demonstrate that sulfuric acid is the most efficient eluent for extracting uranium from the loaded resin, highlighting its potential for use in multiple desorption and recovery cycles. To evaluate the stability and reusability of the resin, six successive sorption-desorption cycles were carried out. The results, summarized in Table 9, demonstrate that the resin performed reliably across all cycles.

3.10. Uranium recovery from leach liquor solution (case study)

To judge the practical applicability of the MTA6002PF resin, uranium recovery experiments were conducted using sulfate leach liquor from El Erediva uranium ore in Egypt. The pH of the leach liquor was adjusted with a buffer solution to optimize the sorption conditions before processing. The experiments were carried out with the following parameters: a shaking time of 240 minutes, room temperature, and resin dosage of 1.0 g/L. The results revealed that the resin achieved a sorption capacity of 63.7 mg/g, which is about 90% of its theoretical capacity.



means of MTA6002PF resin.

60 qe (mg g⁻¹) 40 30

Figure 7. The U(VI) sorption Isotherm by means of MTA6002PF resin.

percentage. Sorption efficiency, 9 90 60 30

Figure 8. The impact of resin dosage on the capture %.

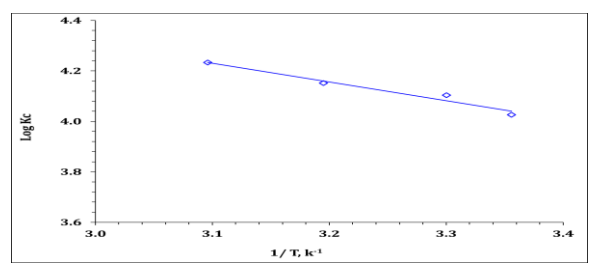


Figure 9. The plot of Van't Hoff for U(VI) sorption by means of MTA6002PF resin.

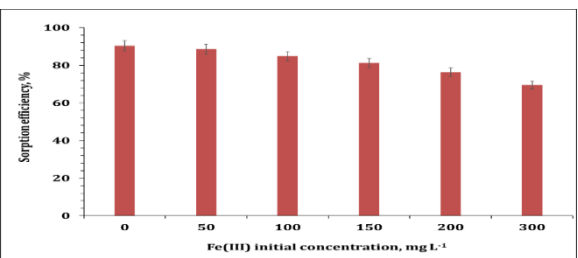


Figure 10. Impact of Fe(III) ions concentration on Uadsorption using MTA6002PF resin.

Name	MTA6002PF
Phys. form	Spherical beads
Matrix	Gel polystyrene cross-linked with divinylbenzene
Funct. Group	Pyridinium
Ionic form (as shipped)	SO ₄ 2-
Tot. Capacity (min.)	1.20 eq/l
Moisture Retention	46-53 %
Mean Size Typical	560± 50μm
Spec. grav.	1.05 g/ml
Temp. Limit Cl	100 °C

representative sample

Component	mg/L	Constituent	mg/ L
Na ₂ O	99.0	Fe_2O_3	1999.2
CaQ	359.1	Al ₂ O ₃	115.1
MgO	270.1	Zn	111.0
SO ₄	579.8	Cu	199.5
P_2O_5	3.70	U	379.0

Table2. Analysis of El-Erediya sulfate solution from

Table 1. The chemical and physical features of Purolite
MTA6002PF resin

Pseudo second-order model			
q 2 (mg/g)	48.5		
$k_2 \times 10^3 (\text{min}^{-1})$	2.98		
h (mol/ g. h)	6.4		
t _{1/2} (h)	7.2		
R 2	0.99		
X^2	0.05		
Pseudo first-order model			
q 1 (mg/g)	43.2		
$k_{\perp} (\text{min}^{-1})$	0.09		
R 2	0.97		
X^2	0.68		
70.11.4.701			

	Stage	I	II
W-M model	$k_i (mg/g min^{1/2})$	6.15	1.09
w-M model	С	5.80	25.0
	R ²	0.96	0.95

Capacity, (mg/

g)

74.4

106

131.58

37.3

51.2

58.8

Ref.

[11]

[12]

[18]

[20]

Table 4. The Weber & Morris kinetic model calculated parameters.

Type

Amberlite IRA-400

Amberlite IR120

Amberjet 1200 H resin

Ambersep 920U Cl

Ambersep 920U SO4

Marathon C

Table 3: The applied kinetic models calculated parameters.

Freundlich model			
k _F (mg g ⁻¹) (mg L ⁻	30.74		
$1/n_F$	0.19		
R 2	0.86		
X^2	7.53		
Langmuir 1	nodel		
k _L (L mg ⁻¹)	0.43		
$q_m (mg g^{-1})$	70.2		
R 2	0.99		
X^2	0.02		
Sips model			
q _S (mg g ⁻¹)	70.3		
k _S (L mg ⁻¹)	0.4		
m _s	1.0		
R 2	0.99		
X^2	0.09		

Purolite MTA6002PF	71	Current study	
Table 6. The uptake capacity of uranium (VI) for the applied			
and other resins			

 Table 5. Langmuir, Sips, and Freundlich isotherm confines
 for uranium sorption.

Table 7: Thermodynamic considerations for U(VI) adsorption using MTA6002PF resin.

ΔS	ΔН	ΔG (kJ/ mol)			
(J/ mol K)	(kJ/ mol)	20 °C	30 °C	40 °C	50 °C
124.6	14.2	-23.0	-23.8	-24.9	-26.2

Table 8. U(VI) desorption from loaded MTA6002PF resin using different solutions (240 min, room temperature; 1.0 g/L).

Eluent	Desorption E., %
H ₂ SO ₄	94.0
HCl	86.5
HNO ₃	90.2

4. Conclusion

This study highlights the effectiveness of the Purolite MTA6002PF strong anion exchange resin in adsorbing uranium (VI) from aqueous solutions. Kinetic analysis indicated that the adsorption process adheres to a pseudo-second-order mechanism, suggesting that chemisorption is the key rate-determining step. Isotherm analysis revealed that the Langmuir model best fits the adsorption data, implying that uranium adsorption occurs as monolayer coverage on a uniform surface. Thermodynamic results confirmed that the process is endothermic, spontaneous, and feasible, with increased efficiency at higher temperatures. Uranium desorption was effectively achieved using 1.0 M sulfuric acid, reaching a recovery rate of 94%. The resin demonstrated consistent performance across multiple sorption-desorption cycles, proving its reusability and suitability for industrial applications. Despite the challenges posed by the sulfate leach liquor from Egyptian ores, the commercial resin proved to be a reliable and efficient material for uranium recovery. These findings subsidize to the improvement of more sustainable and cost-effective methods for uranium extraction, addressing both environmental concerns and industrial needs.

References

- [1] Eliwa, A.A., Khawassek, Y.M. and Ahmed, A.M., 2019. Double purification technique for crude yellowcake, selective dissolving for impurities and liquid–liquid extraction from acetate media. *Radiochemistry*, 61(5), pp. 562–568. https://doi.org/10.1134/S1066362219050072.
- [2] Elzoghby, A.A., Haggag, E.S.A., Roshdy, O.E. et al., 2023. Kaolinite/thiourea-formaldehyde composite for efficient U(VI) sorption from commercial phosphoric acid. *Radiochimica Acta*, 111, pp. 91–103. https://doi.org/10.1515/RACT-2022-0091.
- [3] Wang, B., Deng, C., Ma, W. and Sun, Y., 2021. Modified nanoscale zero-valent iron in persulfate activation for organic pollution remediation: a review. *Environmental Science and Pollution Research*, 28, pp. 34229–34247. https://doi.org/10.1007/S11356-021-13972-W.
- [4] Kamar, M.S., Shalan, A.S., Youssef, W.M., Hussein, A.E.M., Khawassek, Y.M. and Taha, M.H., 2022. Wall rock alteration, uranium mineralization and potentiality of uranium and iron dissolution from mineralized Abu Rusheid gneisses rock, South Eastern Desert, Egypt. *Radiochemistry*, 64(2), pp. 244–256. https://doi.org/10.1134/S1066362222020163.
- [5] Youssef, W.M., Masoud, A.M., Elmaadawy, M.M. and Khawassek, Y.M., 2024. Uranium (VI) sorption from aqueous solution using commercial anion exchange resins; kinetics, isotherm, and thermodynamic investigations. *Journal of Radioanalytical and Nuclear Chemistry*. https://doi.org/10.1007/s10967-024-09438-1.
- [6] Hussein, G.M., 2022. Extraction of thorium (IV) ions from aqueous sulfate media by amino bromo phenyl diazenyl pyrazolo pyrimidinyl cyclohexanone. *International Journal of Environmental Analytical Chemistry*, 102(2), pp. 528–545. https://doi.org/10.1080/03067319.2020.1724982.
- [7] Masoud, A.M., El-Maadawy, M.M., Taha, M.H. and Meawad, A., 2023. Uranium capture from aqueous solution using cement kiln dust; equilibrium and kinetic studies. *Journal of Radioanalytical and Nuclear Chemistry*, 332, pp. 2487–2497. https://doi.org/10.1007/S10967-023-08937-X.
- [8] Masoud, A.M., El-Zahhar, A.A., El Naggar, A.M.A. et al., 2023. Soya bean derived activated carbon as an efficient adsorbent for capture of valuable heavy metals from waste aqueous solution. *Radiochimica Acta*, 111, pp. 105–115. https://doi.org/10.1515/RACT-2022-0098.
- [9] Elzoghby, A.A., Haggag, E.S.A., Roshdy, O.E. et al., 2023. Kaolinite/thiourea-formaldehyde composite for efficient U(VI) sorption from commercial phosphoric acid. *Radiochimica Acta*, 111, pp. 91–103. https://doi.org/10.1515/RACT-2022-0091.
- [10] Sanzharova, N.I., Ratnikov, A.N., Fesenko, S.V. and Sviridenko, D.G., 2019. Review on uranium in soil: levels, migration. *Bulletin of the V.V. Dokuchaev Soil Institute*, 0, pp. 117–132. https://doi.org/10.19047/0136-1694-2019-100-117-132.
- [11] Khawassek, Y.M., 2014. Production of commercial uranium concentrate from El-Sela shear zone mineralized ore material, South Eastern Desert Egypt, at Inshas Pilot Plant Unit. *Nuclear Science and Science Journal*, 3, pp. 169–179. https://doi.org/10.21608/NSSJ.2014.30972.

- [12] Gawad, E.A., 2019. Uranium removal from nitrate solution by cation exchange resin (Amberlite IR 120), adsorption and kinetic characteristics. *Nuclear Science and Science Journal*, 8, pp. 213–230. https://doi.org/10.21608/NSSJ.2019.30142.
- [13] Elzoghby, A.A., 2021. Kinetic and equilibrium studies for U(VI) and Cd(II) sorption from commercial phosphoric acid using C100H resin. *Journal of Radioanalytical and Nuclear Chemistry*, 329, pp. 899–911. https://doi.org/10.1007/S10967-021-07832-7.
- [14] Khawassek, Y.M., Masoud, A.M., Taha, M.H. and Hussein, A.E.M., 2018. Kinetics and thermodynamics of uranium ion adsorption from waste solution using Amberjet 1200H as cation exchanger. *Journal of Radioanalytical and Nuclear Chemistry*, 315, pp. 493–502. https://doi.org/10.1007/S10967-017-5692-1.
- [15] Khawassek, Y.M., 2018. Leaching of uranium from its mineralization and experimental design of the process. *Radiochemistry*, 60(6), pp. 678–684. https://doi.org/10.1134/S1066362218060188.
- [16] Taha, M.H., Masoud, A.M., Khawassek, Y.M., Hussein, A.E.M., Aly, H.F. and Guibal, E., 2020. Cadmium and iron removal from phosphoric acid using commercial resins for purification purpose. *Environmental Science and Pollution Research*, 27, pp. 31278–31288. https://doi.org/10.1007/s11356-020-09342-7.
- [17] Taha, M.H., 2021. Sorption of U(VI), Mn (II), Cu(II), Zn(II), and Cd(II) from multi-component phosphoric acid solutions using MARATHON C resin. *Environmental Science and Pollution Research*, 28, pp. 12475–12489. https://doi.org/10.1007/S11356-020-11256-3.
- [18] Youssef, W.M., 2022. Solid—liquid extraction of uranium from aqueous solution using Marathon C as a strong cation exchanger resin: kinetic, and isotherm studies. *International Journal of Environmental Analytical Chemistry*. https://doi.org/10.1080/03067319.2022.2134995.
- [19] Massoud, A., Masoud, A.M. and Youssef, W.M., 2019. Sorption characteristics of uranium from sulfate leach liquor by commercial strong base anion exchange resins. *Journal of Radioanalytical and Nuclear Chemistry*, 322, pp. 1065–1077. https://doi.org/10.1007/S10967-019-06770-9.
- [20] Massoud, A.M., Khawassek, Y.M., Taha, M.H. and Hussein, A.E.M., 2018. Kinetics and thermodynamics of uranium ions adsorption from acidic aqueous solutions using Amberjet 1200 H as cation exchanger. *Journal of Radioanalytical and Nuclear Chemistry*, 315(3), pp. 493–502. https://doi.org/10.1007/S10967-017-5692-1.